

Coherent Radiation Spectroscopy of Few-Femtosecond Electron Bunches Using a Middle-Infrared Prism Spectrometer

T. J. Maxwell,¹ C. Beherens,^{1,2} Y. Ding,¹ A. S. Fisher,¹ J. Frisch,¹ Z. Huang,¹ and H. Loos¹

¹SLAC National Accelerator Laboratory, Menlo Park, CA 94025, USA

²Deutsches Elektronen-Synchrotron DESY, Notkestraße 85, 22607 Hamburg, Germany

(Dated: July 17, 2013)

Modern, high-brightness electron beams such as those from plasma wakefield accelerators and free-electron laser linacs continue the drive to ever-shorter bunch durations. In low-charge operation (~ 20 pC), bunches shorter than 10 fs are reported at the Linac Coherent Light Source (LCLS). Though suffering from a loss of phase information, spectral diagnostics remain appealing as compact, low-cost bunch duration monitors suitable for deployment in beam dynamics studies and operations instrumentation. Progress in middle-infrared (MIR) imaging has led to the development of a single-shot, MIR prism spectrometer to characterize the corresponding LCLS coherent beam radiation power spectrum for few-femtosecond scale bunch length monitoring. In this letter we report on the spectrometer installation as well as the temporal reconstruction of 3 to 60 fs-long LCLS electron bunch profiles using single-shot coherent transition radiation spectra.

PACS numbers: 29.27.-a, 41.60.Dk, 41.75.Ht

Generation and characterization of femtosecond duration electron bunches are of paramount importance in high-energy collider, plasma wakefield accelerator (PWFA), and x-ray free-electron laser (FELs) applications. In a PWFA, driven by either a laser or an electron bunch, the duration of the accelerated bunch is intrinsically shorter than the plasma oscillation period which is typically on the order of 100 fs [1]. In x-ray FELs, it is understood that reducing the charge per bunch alleviates internal space charge and other nonlinear, beam-induced forces allowing for a corresponding reduction of the minimum possible duration. For example, when operating with tens of picocolomb bunch charges the Linac Coherent Light Source (LCLS) [2] is capable of generating electron and x-ray pulses with durations of just a few femtoseconds [3]. Diagnosis of the longitudinal electron distribution is therefore highly desirable for FEL optimization studies and presents a unique challenge to the resolution of existing diagnostics, reaching into the few-fs scale. In this letter we present first results using a newly developed frequency-domain diagnostic with advantages of economy and robustness over direct time-domain diagnostics [4–6] for the LCLS. The prism-based spectrometer demonstrated yields novel, single-shot measurements over a wide, middle-infrared (MIR) spectral range previously unexplored in longitudinal beam diagnostics.

Frequency-domain bunch length measurements are based on observing the power spectrum of light from an electron bunch undergoing a radiative process, occurring when the beam experiences a change in trajectory or medium [7, 8]. In the low-frequency range, where $\kappa \lesssim (2\pi\sigma_z)^{-1}$ with σ_z the electron bunch length and κ the spatial frequency $\kappa \equiv 1/\lambda$, the radiated power has a well-known coherent enhancement that scales with the number of electrons N over the incoherent beam radiation background. In the one-dimensional bunch limit where the transverse electron beam size is much smaller than the transverse coherence length, the coherent spectral density profile can be expressed as

$$I(\mathbf{r}_\perp, \kappa) \approx N^2 I_e(\mathbf{r}_\perp, \kappa) |f(\kappa)|^2, \quad (1)$$

where the form factor $f(\kappa)$ is defined as the Fourier transform of the unit-normalized longitudinal charge distribution $\rho(z)$ as

$$f(\kappa) = \frac{1}{\sqrt{2\pi}} \int_{-\infty}^{\infty} \rho(z) \exp(2\pi i \kappa z) dz. \quad (2)$$

The function I_e is the spatial distribution in transverse coordinate \mathbf{r}_\perp of spectral component κ for an individual electron. The form of $I_e(\mathbf{r}_\perp, \kappa)$ varies depending on the radiative process and imaging optics used. Coherent transition radiation (CTR) was used for this study, produced when the beam strikes a thin foil. Descriptions of I_e for CTR have been rigorously studied [8–12] with the transverse coherence condition on the beam size $\sigma_r \ll \gamma\lambda/2\pi$ for a beam with Lorentz factor γ . Equation (1) is the basis of CTR spectroscopy as a bunch length diagnostic. The spectrum from the far infrared ($\kappa \rightarrow 0$) through $\kappa \approx (2\pi\sigma_z)^{-1}$ is measured. With σ_z inversely proportional to the measured spectral bandwidth, the increasingly shorter bunches from high-brightness beams demand ever-higher bandwidth spectrometry.

In the LCLS linac, shown in Fig. 1, RF accelerating sections (L0, L1, L2 and L3) bring the beam to a final energy of 3.5–14 GeV prior to reaching the undulator section where ultrashort x-ray pulses are generated. The longitudinal dispersion of bunch compressor chicanes BC1 and BC2 reduce the length of the linearly energy chirped electron bunch. Existing LCLS relative bunch length monitor (BLM) locations are also shown [12, 13]. These record the integrated coherent edge radiation power to provide a relative measure of bunch length. Absolute measurement is achieved by calibrating BLM detector levels at well-defined beam conditions to LCLS transverse deflecting mode cavity measurements.

The minimum achievable σ_z is expected to be $< 10 \mu\text{m}$ at 150 pC, scaling to just $1 \mu\text{m}$ at 20 pC [3]. As σ_z drives the x-ray pulse length generated in the undulator, absolute measurement just prior to the undulator entrance is desired. Small changes to σ_z imparted after BC2 from beam-induced effects (e.g., space charge and wakefields) combined with the weak

Submitted to *Physical Review Letters*.

Work supported in part by US Department of Energy under contract DE-AC02-76SF00515.

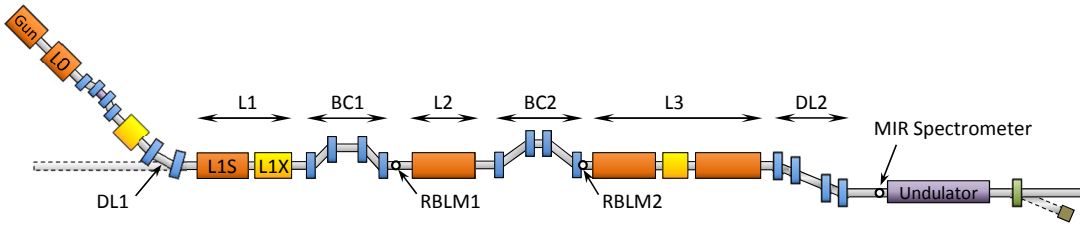


FIG. 1: Layout of the LCLS beamline with locations of relevant diagnostics along the LCLS linac (see text).

dispersion of the dogleg DL2 (Fig. 1) can then be observed.

Single-shot spectroscopy of the MIR coherent beam radiation spanning $\lambda = 1 - 40 \mu\text{m}$ is therefore needed to absolutely determine σ_z over the range of achievable bunch lengths. Many instruments have evolved to characterize CTR for longer wavelengths and were considered for extension down to the few- μm bunch regime [14–21].

To cover the broad MIR range, we have combined the bandwidth of the cascaded grating configuration [21] with the reduced complexity of the single-grating polychromator [19, 20] by using a conventional prism spectrometer design. The weaker, harmonic-independent prism dispersion make wide bandwidth coverage straightforward without the need for order sorting. Tradeoffs for choosing a prism over gratings are lower spectral resolution and the dispersion non-linearity introduced by the prism material properties.

Details on the MIR spectrometer design have been previously discussed [22] with the final system described in Fig. 2. The optics are enclosed and purged to $< 0.1\%$ relative humidity with dried air to minimize atmospheric water vapor absorption bands. The 10° apex-angle prism (H) was fabricated from thallium bromiodide (KRS-5) owing to its flat transmission and strong dispersion over the $\lambda = 0.8 - 40 \mu\text{m}$ range. Reflective optics are used otherwise and chosen to provide diffraction-limited imaging at the linear detector array (J) which consists of 128 lead zirconate titanate (PZT) pyroelectric elements with $100 \mu\text{m}$ spacing.

Calibration is complicated by the relative scarcity of bright MIR sources. Wavelength calibration was performed using an 18 W, 1200°C silicon nitride blackbody source. A series of bandpass filters were used to generate spectral lines. The radiator provided measurable illumination over the range $\lambda = 1.6 - 16 \mu\text{m}$ after chopping, collimation and filtering.

For interpolation and extrapolation of the position x on the array for a given spectral component κ , a curve was fit to the ideal function $x_{calc}(\kappa)$ calculated from Snell’s law for the KRS-5 index of refraction [23] with additional slope and offset parameters allowed for small detector misalignment and an arbitrary spatial offset of the array. The FWHM spectral resolution $\Delta\kappa$ is computed from the spatial dispersion $dx/d\kappa$ as $\Delta\kappa \approx (dx/d\kappa)^{-1} \Delta x$, where Δx is the diffraction-limited image of the slit at the detector. Results are shown in Fig. 3.

Accurate bunch length determination is predicated on characterizing the total spectral amplitude transfer function $T(\kappa)$ for the system. Where the transverse extent of spectral com-

ponents can be neglected, the measured spatial power density $I_{meas}[x(\kappa)]$ along coordinate x at the array is approximately related to the term $|f(\kappa)|^2$ via several contributing factors as

$$\begin{aligned} I_{meas}[x(\kappa)] &= (dx/d\kappa)^{-1} T_{det}(\kappa) T_{abs}(\kappa) [I_e(\kappa) |f(\kappa)|^2] \\ &= T(\kappa) |f(\kappa)|^2. \end{aligned} \quad (3)$$

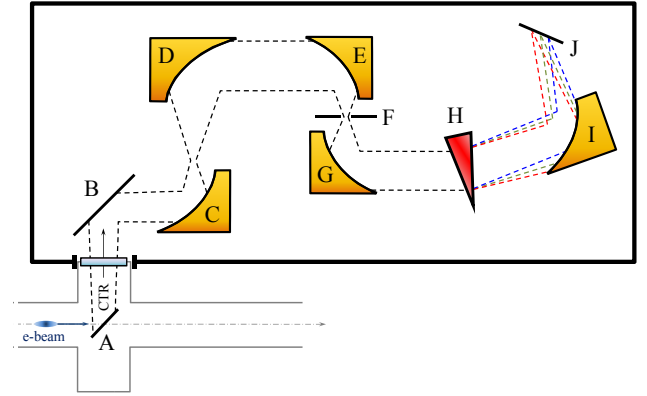


FIG. 2: Schematic for MIR spectroscopy of CTR with CTR envelope shown as dashed lines. CTR from a thin foil inserted into the electron beam (A) is imaged with reflective optics ($B - E$) to the spectrometer entrance slit (F), chromatically dispersed by a custom KRS-5 prism (H), then spectrally resolved on a linear detector array (J).

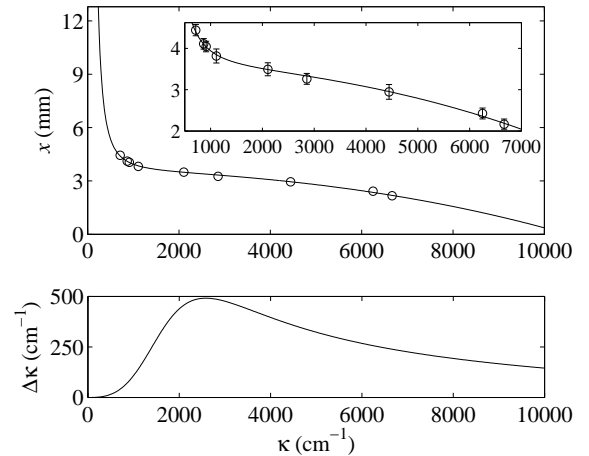


FIG. 3: Fit of computed detector position x as a function of spatial frequency κ to a sample of spectral lines (top) with detail view on sampled points (top, inset) and spectral resolution $\Delta\kappa$ (bottom).

The dx/dk term represents the nonlinear mapping of the spectral density to the measured spatial density via the dispersion. Other terms are the detector response T_{det} [16, 21], the spatially-integrated single electron imaging contribution $I_e(\kappa)$ from Eq. (1), and T_{abs} from absorption by the prism and the vacuum and detector windows.

Data using the incoherent blackbody source lacked the resolution and spectral range for accurate amplitude calibration. A procedure is being refined using the Advanced Light Source (ALS) MIR Beamline to address this [24]. Where the beam being diagnosed is the only readily available coherent MIR source, an online approach was used to reconstruct $T(\kappa)$ and is discussed here.

Assume the electron beam can be used to generate several MIR spectra by changing any independent accelerator parameter ϕ that will generate a different longitudinal distribution $\rho(z; \phi)$. Then we can measure a 2D spectral intensity function

$$I_{meas}(\kappa; \phi) = T(\kappa) |f_{meas}(\kappa; \phi)|^2, \quad (4)$$

where the instrument response T is independent of ϕ if I_e is not significantly affected by ϕ . If we can reasonably simulate the electron beam's dependence on ϕ to generate $|f_{sim}(\kappa; \phi)|^2$, scale factors $T(\kappa)$ can be fit to satisfy Eq. (4). This tenuously assumes the spectra are sufficiently varied so that the ϕ and κ dependencies can be separated.

A natural candidate for the independent parameter is the RF phase ϕ_{L2} of accelerating section L2 just prior to BC2 (Fig. 1). Changing ϕ_{L2} changes the energy chirp put on the bunch prior to compression so that the resulting bunch length is varied. During this ‘‘chirp scan’’ the RF amplitude V_{L2} is adjusted so the energy gain $E_{L2} = V_{L2} \cos \phi_{L2}$ is kept constant.

Scans were simulated using the *LiTrack* fast longitudinal phase space tracking and wakefield solver [25]. Unknown offsets to experimental settings are left free to improve fitting including the initial bunch energy spread, length and chirp, and the accelerator RF phases and amplitudes. Longitudinal profiles $\rho(z; \phi)$ are simulated and Fourier transformed to $|f_{sim}(\kappa; \phi)|^2$. A steepest-descent method is used to minimize the least-squares difference between simulated CTR spectra $|f_{sim}|^2$ and the corrected measured spectra $|f_{meas}|^2 = I_{meas}/T$ with respect to simulation parameters, then minimized with respect to $T(\kappa)$ before the process repeats.

Chirp scan data for fitting was collected at LCLS with an electron beam energy of 13.4 GeV and 40 pC bunch charge. The scan was performed around maximum beam compression so the minimum expected bunch length is $\sim 2 \mu\text{m}$, providing CTR across the full spectrometer range. Results are shown in Fig. 4 including I_{meas} , best candidates for I_{sim} and T , and corrected data $f_{meas} = I_{meas}/T$.

In $T(\kappa)$ a pile up is observed around 3000 cm^{-1} from the bottoming out of the dx/dk dispersion contribution [Eq. (3), Fig. 3]. Periodic minima every 2000 cm^{-1} in κ (with additional structure) are also seen in parallel tests at the ALS MIR Beamline (without structure), consistent with thin-film interference in the $1.5 \mu\text{m}$ -thick PZT layer of the detector array.

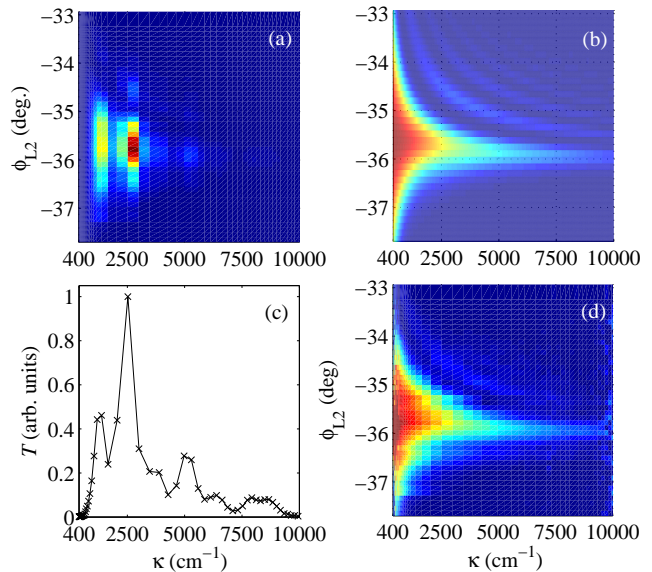


FIG. 4: $T(\kappa)$ reconstruction results for an L2 chirp scan of a 40 pC bunch with (a) raw data $I_{meas}(\kappa; \phi_{L2})$, best fit solutions for (b) $|f_{sim}(\kappa; \phi)|^2$ and (c) transmission function $T(\kappa)$, and (d) final corrected spectra $|f_{meas}(\kappa; \phi_{L2})|^2 = I_{meas}(\kappa; \phi_{L2})/T(\kappa)$.

Minimum bunch length (maximum bandwidth) in Fig. 4 corresponds to the full-compression phase $\phi_{full} = -36^\circ$. A ϕ_{L2} -dependent spectral ringing structure appears in both simulation and the $T(\kappa)$ -corrected data where $|\phi_{L2}| < |\phi_{full}|$ showing excellent agreement.

With $x(\kappa)$ and $T(\kappa)$ characterized, we would like to use measured spectral profiles to retrieve the longitudinal profiles $\rho(z)$. However, the spectral phase is unknown so the inverse Fourier transform to $\rho(z)$ cannot be uniquely determined. Common in CTR bunch length measurements [16, 17, 21], the minimum Kramers-Kronig phase ϕ_{min} is reconstructed following the prescription in [26–28]. This solution is still non-unique, and it is understood that ambiguities remain (cf. [28]). Several methods for low- κ and high- κ completion of measured spectra were analyzed where required. The choice of these was not found to significantly impact the results shown here.

Example reconstructions are shown in Fig. 5 for the typical LCLS hard x-ray mode with a 13.4 GeV, 150 pC beam. Bunch length was again varied by changing the L2 RF phase with four examples shown: two of the under-compressed beam ($|\phi_{L2}| < |\phi_{full}|$), one at full compression, and one over compressed ($|\phi_{L2}| > |\phi_{full}|$). Spectrum curves are cubic interpolants of the measured points to provide over sampling for phase reconstruction. Due to the weak transmission for $\kappa \lesssim 500 \text{ cm}^{-1}$ (see Fig. 4), these points are discarded for interpolation. Points at $\kappa = 0$ are inferred from the locally measured bunch charge. The curves are used to retrieve ϕ_{min} which is used to invert the Fourier transform, recovering $\rho(z)$.

The beam currents $I(z) = Q\rho(z)$ are shown in Fig. 5, bottom, with corresponding FWHM bunch lengths Δz . For both

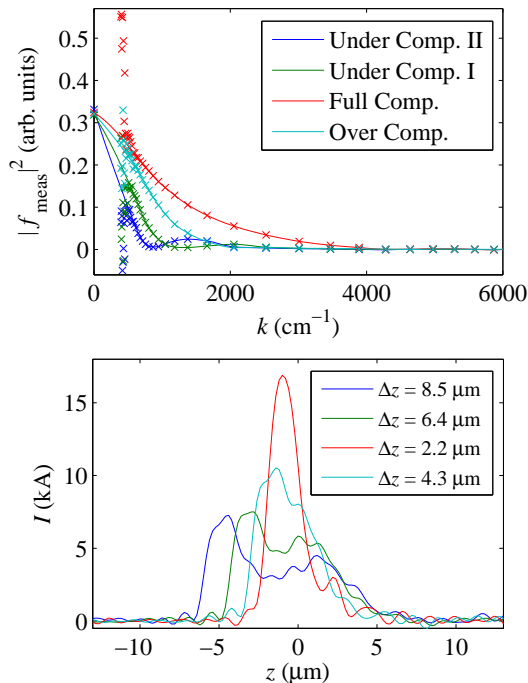


FIG. 5: Example beam profile reconstruction for 13.4 GeV, 150 pC electron bunches at four different L2 RF phase settings around full compression showing (a) data and interpolants with (b) resulting current profiles and true FWHM bunch lengths Δz .

under-compressed cases, an expected double-horn structure appears in the currents showing small head and tail bumps [3].

The reconstruction procedure was applied to the full range of the chirp scan from which these examples were taken. A simulated phase scan using the set machine parameters was also performed. These are shown in Fig. 6 and compared to simultaneous BLM2 measurements (Fig. 1). Note that no fitting between simulation and measurement was applied.

As BLM2 is calibrated assuming a square pulse, the values Δz in Fig. 6 are from square-pulse fitting of all beam current profiles. The spectrometer agrees well with simulation with both having minima of $5.0 \mu\text{m}$. Full compression phases from the spectrometer and BLM2 are $\phi_{full} = -39.0^\circ$ and -38.4° , respectively, illustrating the difference in bunch length at BC2 and the undulator entrance. Curves converge around $\phi_{L2} = -36^\circ$. This is the typical set point for LCLS operations expected to provide minimum projected electron energy spread and corresponds to the under compressed II case in Fig. 5. The minimum Δz of $17 \mu\text{m}$ for BLM2 is from a $30 \mu\text{m}$ long-pass filter used to block optical wavelengths. The deviation of the spectrometer result for $\Delta z > 18 \mu\text{m}$ stems from poor sensitivity for $\kappa < 500 \text{ cm}^{-1}$ ($\lambda > 20 \mu\text{m}$).

The MIR spectrometer performs well in the shorter bunch regime. Pursuant to low-charge studies, analysis of scans for 20 and 10 pC bunch charges yield minimum FWHM bunch lengths Δz of 1.3 and $0.7 \mu\text{m}$, respectively. In these cases, however, extrapolation of the high- κ tail beyond the spectrom-

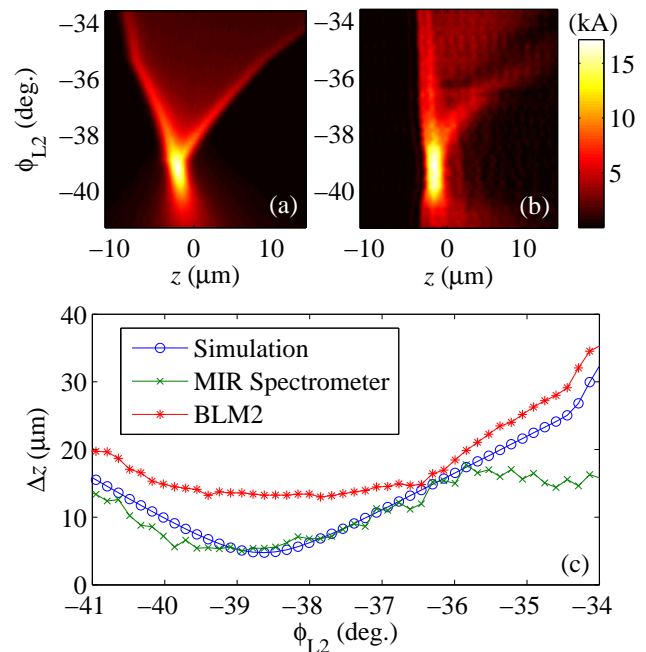


FIG. 6: Comparisons for the beam current profile dependence on L2 RF phase for a 13.4 GeV, 150 pC electron bunch with (a) simulated profiles as a function of ϕ_{L2} , (b) profiles reconstructed from measured MIR spectra, and (c) FWHM bunch lengths Δz from square current profile fitting including LCLS BLM2 measurement.

eter $\kappa = 9000 \text{ cm}^{-1}$ cutoff is required. Furthermore the signal levels begin to approach the noise level of the detector array.

Improvements continue to push both long- and short-bunch boundaries. In the short-bunch limit a silicon filter window on the detector cuts off near-IR wavelengths to prevent photocurrent generation in the integrated circuit. A sensor without this requirement is being evaluated to both extend the spectrometer below $1 \mu\text{m}$ and double the intensity of light reaching the array making $< 10 \text{ pC}$ bunch profile measurements possible. For longer bunches, zinc selenide (ZnSe) neutral density filters were used to attenuate the CTR that saturates the array for $Q \gtrsim 40 \text{ pC}$. Though the filter transmission has been measured to be flat over the spectrometer range [24], it absorbs strongly for $\kappa < 500 \text{ cm}^{-1}$, worsening transmission in this range. KRS-5 neutral density filters are being explored to improve this.

In summary, a novel, compact, MIR prism spectrometer has been designed, calibrated and successfully demonstrated as a single-shot bunch length monitor for the LCLS. A combination of beam- and simulation-based spectrometer characterization was demonstrated partially circumventing the need for an additional MIR source. Though not an ideal or independent solution, this approach naturally accounts for all spectral effects present in the system including difficult to quantify CTR imaging contributions. While demonstrated using CTR, non-interceptive processes such as coherent edge or diffraction radiation can be used to make it an online diagnostic.

Initial performance has been compared to independent

measurement and simulation. Combining measured spectra with longitudinal profile reconstruction, bunch structure is resolved with reasonable agreement to simulation. Bunch durations spanning 0.7 – 18 μm over a range from 10 – 150 pC have been observed, exceeding design expectations in the low-charge, short-bunch regime. Already integrated with LCLS, this MIR spectrometer continues to operate in support of FEL performance improvement studies.

We thank Axel Brachmann, Franz-Josef Decker, Sasha Gilevich, Rick Iverson, Gene Kraft, Jennifer Loos, Agostino Marinelli, Mike Minitti, Joe Robinson, Jim Turner of SLAC National Accelerator Laboratory for their valuable contributions and support. This work was supported in part by US Department of Energy contract number DE-AC02-76SF00515.

-
- [1] E. Esarey, C. B. Schroeder, and W. P. Leemans, *Rev. Mod. Phys.* **81**, 1229 (2009).
- [2] P. Emma *et al.*, *Nature Photonics* **4**, 641 (2010).
- [3] Y. Ding *et al.*, *Phys. Rev. Lett.* **102**, 254801 (2009).
- [4] Y. Ding *et al.*, *Phys. Rev. ST Accel. Beams* **14**, 120701 (2011).
- [5] P. Emma, J. Frisch, and P. Krejcik, “A Transverse RF Deflecting Structure for Bunch Length and Phase Space Diagnostics,” SLAC Technical Note LCLS-TN-00-12 (2000).
- [6] P. Krejcik *et al.*, in *Proc. of 2012 Int. Beam Instrum. Conf.* (Tsukuba, Japan, 2012) p. TUPA41.
- [7] J. D. Jackson, *Classical Electrodynamics*, 3rd ed. (Wiley, New York, 1998).
- [8] V. Ginzburg and I. Frank, *J. Phys. USSR* **9**, 353 (1945).
- [9] S. Casalbuoni, B. Schmidt, P. Schmüser, V. Arsov, and S. Wesch, *Phys. Rev. ST Accel. Beams* **12**, 030705 (2009).
- [10] M. Castellano, A. Cianchi, G. Orlandi, and V. A. Verzilov, *Nucl. Instrum. Meth. A* **435**, 297 (1999).
- [11] A. G. Shkvarunets and R. B. Fiorito, *Phys. Rev. ST Accel. Beams* **11**, 012801 (2008).
- [12] H. Loos, T. Borden, P. Emma, J. Frisch, and J. Wu, in *Proc. of 2007 IEEE Part. Accel. Conf.* (Albuquerque, New Mexico, 2007) pp. 4189–4191.
- [13] M. Dunning *et al.*, *Int. J. of Mod. Phys. A* **22**, 4125 (2007).
- [14] H.-c. Lihn, P. Kung, C. Settakorn, H. Wiedemann, and D. Bock, *Phys. Rev. E* **53**, 6413 (1996).
- [15] A. Murokh *et al.*, *Nucl. Instrum. Meth. A* **410**, 452 (1998).
- [16] D. Mihalcea, C. L. Bohn, U. Happek, and P. Piot, *Phys. Rev. ST Accel. Beams* **9**, 082801 (2006).
- [17] L. Frölich, “Bunch Length Measurements Using a Martin-Puplett Interferometer at the VUV-FEL,” DESY-THESIS 2005-11 (2005).
- [18] J. Thangaraj *et al.*, *Rev. Sci. Instrum.* **83**, 043302 (2012).
- [19] Y. Sugiyama, Y. Shibata, S. Sasaki, K. Ishi, T. Tsutaya, T. Osaka, M. Ikezawa, M. Oyamada, and Y. Kondo, *Bull. Res. I. Sci. Meas., Tohoku Univ* **48**, 1 (1999).
- [20] T. Watanabe *et al.*, *Nucl. Instr. and Meth. A* **480**, 315 (2002).
- [21] S. Wesch, B. Schmidt, C. Behrens, D.-H. Hossein, and P. Schmuüser, *Nucl. Instr. Meth. A* **665**, 40 (2011).
- [22] T. Maxwell, Y. Ding, A. Fisher, J. Frisch, and H. Loos, in *Proc. of 2012 Int. Beam Instrum. Conf.* (Tsukuba, Japan, 2012) p. TUPA47.
- [23] W. S. Rodney and I. H. Maliston, *J. Opt. Soc. Am.* **46**, 956 (1956).
- [24] M. Martin, Advanced Light Source, Lawrence Berkeley National Laboratory, Berkeley, CA, personal communication (2013).
- [25] K. Bane and P. Emma, in *Proc. of 2005 IEEE Particle Accel. Conf.* (Knoxville, Tennessee, 2005) pp. 4266–4268.
- [26] J. S. Toll, *Phys. Rev.* **104**, 1760 (1956).
- [27] R. Lai and A. Sievers, *Phys. Rev. E* **50**, 3342 (1994).
- [28] R. Lai and A. Sievers, *Nucl. Instrum. Meth. A* **397**, 221 (1997).